Journal of Luminescence 192 (2017) 263–268

Contents lists available at ScienceDirect

Journal of Luminescence

journal homepage: www.elsevier.com/locate/jlumin

Investigation of europium concentration dependence on the luminescent properties of borogermanate glasses

Melis Gökçe[a,*], Ufuk Şentürk[b], Deniz K. Uslu[a], Gözde Burgaz[a], Yüksel Şahin[c], Aytaç Gürhan Gökçe[d]

[a] Department of Physics, Adnan Menderes University, Aydın 09010, Turkey
[b] Department of Materials Science and Engineering, Izmir Institute of Technology, İzmir 35430, Turkey
[c] Department of Chemistry, Adnan Menderes University, Aydın 09010, Turkey
[d] Department of Physics, Dokuz Eylül University, İzmir 35160, Turkey

ARTICLE INFO

Keywords:
Borogermanate glass
Europium
Luminescence
Judd-Ofelt
Decay time

ABSTRACT

In order to elucidate the effect of europium content on the optical and luminescent properties of borogermanate glasses, a series of Eu^{3+} doped $30B_2O_3$-$40GeO_2$-(30-x)Gd_2O_3 glasses with various doping levels (x = 1–9 mol%) have been synthesized and studied with transmission, absorption, photoluminescence and decay time measurements. The transmission spectra proved that the title glasses maintained a high transparency about 80% in the 440 to 900 nm region. Based on the absorption spectra, the optical band gaps obtained from Tauc's plot can be narrowed by increasing content of Eu^{3+}. From the photoluminescence spectra, the strongest red emission has been observed from the $^5D_0 \rightarrow {}^7F_2$ level of Eu^{3+} ions in borogermanate glasses. The strongest emission and excitation intensities of Eu^{3+} ions are at the doping level of x = 7 mol% and then these intensities decrease due to concentration quenching. The red to orange ratio (R/O) of $^5D_0 \rightarrow {}^7F_2$ to $^5D_0 \rightarrow {}^7F_1$ transitions has been investigated to predict the local environment of Eu^{3+} ions. Judd-Ofelt (J-O) analyses have been performed from the emission spectra. The values of R/O and Ω_2 present an increase with increasing doping level, indicating the lower symmetric environment for Eu^{3+} ions and higher covalency for Eu-O bond. The emission efficiency calculated from J-O theory is 75% at x = 2 mol%. The decay time curves of $^6P_{7/2} \rightarrow {}^8S_{7/2}$ transition of Gd^{3+} ions and $^5D_0$–$^7F_2$ transition of Eu^{3+} ions confirm the energy transfer from Gd^{3+} to Eu^{3+} ions.

1. Introduction

Due to their unique optical properties, rare earth (RE) doped glasses are very attractive materials for diverse optical devices, such as advanced laser materials, plasma displays, optical waveguides, fiber amplifiers, efficient upconverters [1–4]. For the highest performance for these devices the optical properties of RE ions must be correlated with their local environment in detail [5]. In order to develop new optical devices borate, silicate and phosphate glass systems have been studied as host materials for the incorporation of trivalent RE ions [6]. In view of their high RE ion solution capacity, high thermal stability, high transparency, lower melting point, lower phonon energy, ease of shaping and low cost properties, borogermanate glasses surpass phosphate, silicate or borosilicate glass systems [7–9]. Borogermanate glasses have been used in several application areas that include scintillators, solar cells, solid state lasers and glass fibers [10–13]. Within other RE elements, Eu^{3+} ions are very effective in the investigation of the local environment of the glass materials, owing to its relatively simple energy level and hypersensitive $^7F_0 \rightarrow {}^5D_2$ transition [5,14]. Because of the properties stated above research have been conducted on Eu^{3+} doped borogermanate systems [15–17].

Glass systems doped with Gd^{3+} have been studied for various applications such as medical therapy [18], scintillator [19] and x-ray imaging [20]. In addition Gd^{3+} ion has been studied due to its significant importance in the efficient energy transfer to the incorporated ions (such as Eu^{3+}) [20–25]. Luminescent properties of glasses can be improved by energy transfer between these ions [20,26,27].

In the present work a series of europium-gadolinium co-doped borogernanate glasses have been designed for use as glass scintillators. The structural analyses of these glasses have been determined by x-ray diffraction (XRD) and Fourier transform infrared (FTIR) measurements. Absorption, transmittance, photoluminescence (PL) spectra, Judd–Ofelt analysis and decay time measurements have been evaluated in order to obtain optical and luminescent properties of borogermanate glasses as a function of Eu^{3+} concentration.

* Corresponding author.
E-mail address: mgokce@adu.edu.tr (M. Gökçe).

http://dx.doi.org/10.1016/j.jlumin.2017.06.041
Received 18 April 2017; Received in revised form 16 June 2017; Accepted 19 June 2017
Available online 23 June 2017

2. Experimental methods

The glasses with composition of $30B_2O_3$-$40GeO_2$-(30-x)Gd_2O_3-xEu_2O_3 (x = 1,2,3,5,7,9 mol%; labeled as BGGEx) have been prepared by melt quenching method. The raw materials used for the prepared glasses were H_3BO_3 (99.99%, Alfa Aesar), GeO_2 (> 99.99%, Aldrich), Gd_2O_3 (99.9%, Aldrich) and Eu_2O_3 (99.9%, Aldrich). About 10 g batches were mixed by grinding homogeneously in an agate mortar and melted in an alumina crucible under air atmosphere at 1300~1400 °C for 3 h. The melt was poured onto a preheated stainless steel plate and pressed by another plate and then annealed at 550–600 °C for 6 h to release internal stresses and avoid cracking of the sample. Optical measurements were done on the polished glass samples with a thickness about 2.5 mm. XRD measurements were carried out using Rigaku-Rint 2200/PC (Ultima 3) diffractometer in the range of 10° and 90°. The FTIR spectrum was recorded using Perkin-Elmer BX-II FTIR spectrometer in the range of 400–4000 cm^{-1}. The glass densities were determined according to the Archimedes principle by using distilled water as an immersion liquid. Absorption and transmittance spectra were measured on a Perkin-Elmer Lambda 25 UV–vis spectrometer. The photoluminescence excitation and emission spectra were recorded by FluoroMax-4 (Horiba Jobin Yvon) spectrofluorometer equipped with a 150 W xenon lamp source. The decay time measurements were carried out using a Time Correlated Single Photon Counting (TCSPC) system (Edinburgh Instruments) with a micro second flash lamp as an excitation source. All the measurements were carried out at room temperature.

3. Results and discussion

Various physical properties including molecular weight (M), density (ρ), refractive index (n), molar volume (V_m), packing density (PD), rare earth-ion concentration (N), polaron radius (r_p) and critical distance (R_c) for Eu^{3+} doped borogermanate glasses have been provided in Table 1. The refractive indexes of glasses have been calculated using Gladstone-Dale relation [28]. The critical distances (R_c) and other calculated physical properties of glasses have been obtained according to literature [29,30], respectively.

As the molecular mass of Eu^{3+} ion is less than Gd^{3+} ion, the glass density decreases gradually by the increase in content of Eu^{3+} ions. The critical distance between Eu^{3+} ions is higher than the polaron radius for all samples. Both the values of R_c and r_p reduce with the increase of Eu^{3+} ion content [22]).

3.1. Structural analysis

The XRD pattern of x = 1 mol% Eu^{3+} doped borogermanate glass is shown in Fig. 1. The spectrum exhibits a broad scattering at around 25° and 55° and lacks the presence of specific crystalline peaks, indicating the amorphous nature of network structure.

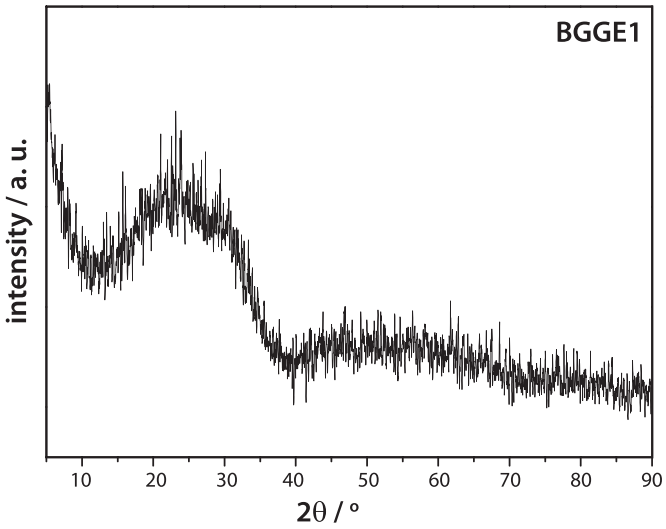

Fig. 1. XRD pattern of BGGE1 glass.

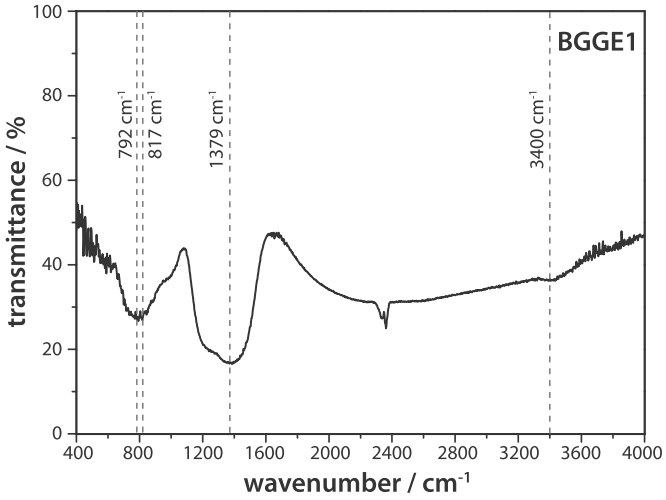

Fig. 2. Infrared transmission spectrum of BGGE1 glass.

As a representative case, the IR spectra of BGGE1 glass (Fig. 2) has been evaluated to identify the structural formation. The typical absorption band of OH^- group is centered at 3400 cm^{-1}, which reveals

Table 1
The digital photographs, molecular weight (M), density (ρ), refractive index (n), molar volume (V_m), packing density (PD), rare earth-ion concentration (N), polaron radius (r_p) and critical distance (R_c).

	BGGE1	BGGE2	BGGE3	BGGE5	BGGE7	BGGE9
						
M (g/mol)	171.585	171.279	171.173	170.962	170.751	170.539
ρ (g/cm^3)	4.807	4.824	4.818	4.764	4.778	4.732
n	1.700	1.702	1.701	1.693	1.695	1.689
V_M (cm^3/mol)	35.694	35.505	35.527	35.886	35.736	36.039
PD (x10^{22} ions/cm^3)	1.687	1.696	1.695	1.678	1.685	1.671
N (x10^{20} ions/cm^3)	1.687	3.392	5.085	8.390	11.795	15.038
r_p (Å)	7.292	5.777	5.048	4.272	3.813	3.516
R_c (Eu^{+3}-Eu^{+3}) (Å)	14.364	11.380	9.943	8.415	7.511	6.927
R_c (Gd^{+3}-Eu^{+3}) (Å)	4.622	4.614	4.615	4.631	4.624	4.637

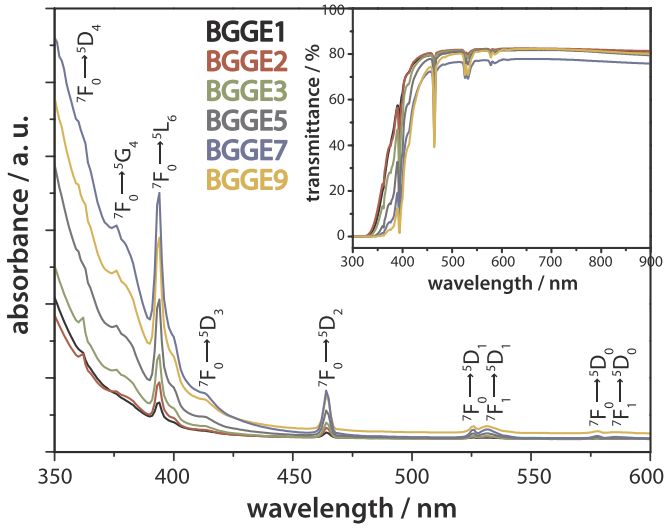

Fig. 3. Optical absorption spectra of BGGEx glasses over the spectral region of 350–600 nm. The inset shows the transmission spectra in the spectral region of 300–900 nm.

the presence of hydroxyl groups in the glass. The broad band observed at 1200–1600 cm^{-1} centered at around 1379 cm^{-1} is attributed to stretching vibrations of BO_3 units with non-bridging oxygen (NBO). The strong absorption bands at 792 and 817 cm^{-1} are characteristic of bending and stretching vibrations of T-O-T (T = B, Ge) linkages [31,32].

3.2. Absorption and transmittance spectra

The absorption and transmittance spectra of $30B_2O_3$–$40GeO_2$–(30-x)Gd_2O_3–xEu_2O_3 borogermanate glasses in the UV–vis regions are presented in Fig. 3. The absorption bands in the spectrum correspond to the 4f–4f optical transitions between the ground and the excited states of the Eu^{3+} ions [5].

The characteristic absorption peaks at 361, 376, 393, 413, 463, 525 and 577 nm are related to optical transitions from $^7F_0 \rightarrow {}^5D_4$, $^5G_4$, $^5L_6$, $^5D_3$, $^5D_2$, $^5D_1$ and $^5D_0$, respectively. Optical transitions from $^7F_1$ to $^5D_1$ and $^5D_0$ states of Eu^{3+} ions are associated with 531 and 588 nm, respectively [33]. In this spectrum, $^7F_0 \rightarrow {}^5L_6$ transition of the absorption peak at 393 nm is found to be more intense than other transitions. The $^7F_0 \rightarrow {}^5D_4$, $^5G_4$, $^5D_3$ transitions exhibit weak intensity, though $^7F_0 \rightarrow {}^5D_3$ transition is forbidden by the ΔJ selection rule. The transition of $^7F_0 \rightarrow {}^5D_0$ is spin-forbidden while the $^7F_0 \rightarrow {}^5D_1$ is magnetic dipole allowed. Notably, the intensity of peaks becomes more evident at higher Eu^{3+} ion content. The transitions below 352 nm cannot be seen in the transmittance spectra, because the cut-off edge of the glasses goes to higher wavelength and the absorption peaks (273, 301, 311 nm) of Gd^{3+} ion disappears. Remarkably all BGGEx glasses show a relatively flat transmittance coefficient within 78–82% range in the 440–900 nm wavelength regions. This is of significance in the higher light-yield output and high transparency for red emission of Eu^{3+} ions [34].

From absorption spectra (Fig.3) the optical band gap (E_g) of BGGEx glasses can be calculated by using the well-known equation, as proposed by Tauc and Menth [35]:

$$\alpha h\upsilon = B(h\upsilon - E_g)^m$$

where hυ is the incident photon energy, B is constant, m is a parameter which depends on the type of electronic transition responsible for absorption. m has values of 1/2 and 2, which correspond to direct and indirect allowed transitions, respectively. The absorption coefficient α can be defined as the ratio of absorbance and thickness. Therefore, by plotting $(\alpha h\upsilon)^{1/m}$ vs. photon energy (Tauc's plot) the optical band gap can be determined from the extrapolation of the linear region of $(\alpha h\upsilon)^{1/m} = 0$. As shown in Table 2, the calculated direct (E_g^d) and indirect (E_g^i) band gaps are in the range between 3.66–3.28 and 3.22–2.84 eV, respectively. Band gap narrowing in BGGEx glasses is observed with the increase of Eu^{3+} doping concentration. This result can be attributed to the fact that the incorporation of more Eu^{3+} ions opens the glass network and generates more NBO [27]. This may also be an explanation for the shift of cut-off edge toward longer wavelengths with the increase Eu^{3+} content.

Table 2
The wavelength cut-off edge ($\lambda_{cut-off}$) and optical band gap values for direct (E_g^d) and indirect (E_g^i) allowed transitions of Eu^{3+} doped borogermanate glasses.

	BGGE1	BGGE2	BGGE3	BGGE5	BGGE7	BGGE9
$\lambda_{cut-off}$ (nm)	324.88	326.73	331.28	342.09	348.06	352.18
E_g^d (eV)	3.66	3.64	3.60	3.48	3.38	3.28
E_g^i (eV)	3.22	3.21	3.17	3.07	2.88	2.84

3.3. Excitation and emission spectra

Photoluminescence (PL) analysis provides valuable information about the optical properties of the sample. PL characterization has been performed in two parts: the emission and excitation spectrum. The excitation spectrum of Eu^{3+} doped borogermanate glasses were obtained by monitoring the $^5D_0 \rightarrow {}^7F_2$ transition of Eu^{3+} ions as shown in Fig. 4. The inset of Fig. 4 shows the 230–300 nm region of the spectrum where the excitation spectra is seen to compose of one broad band in 230–320 nm region and several sharp peaks in 310–600 nm region. Charge-transfer (CT) mechanism from the filled 2p shell of the O^{2-} ligand to the partially field f shell of Eu^{3+} ions is responsible for the formation of this broad band [36]. The characteristic excitation peaks of Gd^{3+} ions at 253 nm ($^8S_{7/2} \rightarrow {}^6D_{9/2}$), 273 nm ($^8S_{7/2}$-$^6I_{11/2}$), 298 nm ($^8S_{7/2}$-$^6P_{5/2}$) and 311 nm ($^8S_{7/2}$-$^6P_{7/2}$) and Eu^{3+} 318 nm ($^7F_0$-^5H_J) are located on the broad CT band. This situation demonstrates the energy transfer from Gd^{3+} to Eu^{3+} ions in such a way that Gd^{3+} ions can absorb the energy at 273 and 311 nm, and then transfer to Eu^{3+} ions [37]. The other sharp peaks lying at 362 nm ($^7F_0 \rightarrow {}^5D_4$), 380 nm ($^7F_0 \rightarrow {}^5G_4$), 393 nm ($^7F_0 \rightarrow {}^5L_6$), 413 nm ($^7F_0 \rightarrow {}^5D_3$), 463 nm ($^7F_0 \rightarrow {}^5D_2$), 530 nm ($^7F_0 \rightarrow {}^5D_1$) and 577 nm ($^7F_0 \rightarrow {}^5D_0$) are related to the intra-4f forbidden transitions of Eu^{3+} ions between the ground and the excited states of $4f^6$ configuration [20,33]. The highest intensity in the

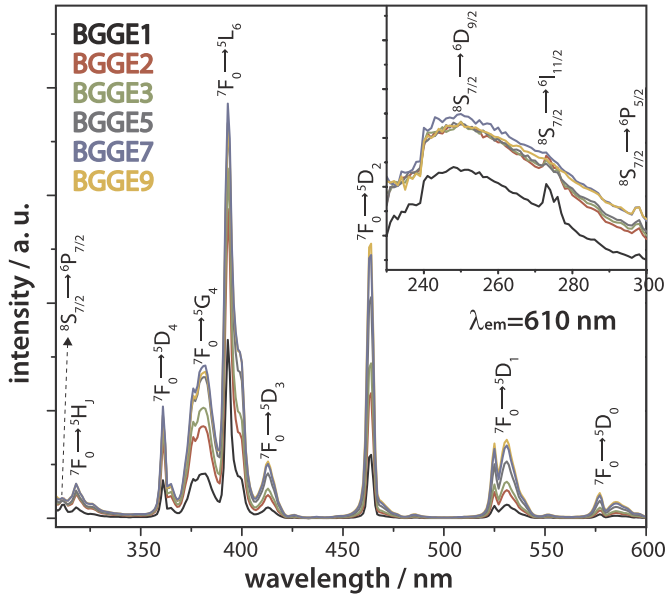

Fig. 4. Excitation spectra of BGGEx glasses. Inset shows the zoom of the excitation spectra in the spectral range of 230–300 nm.

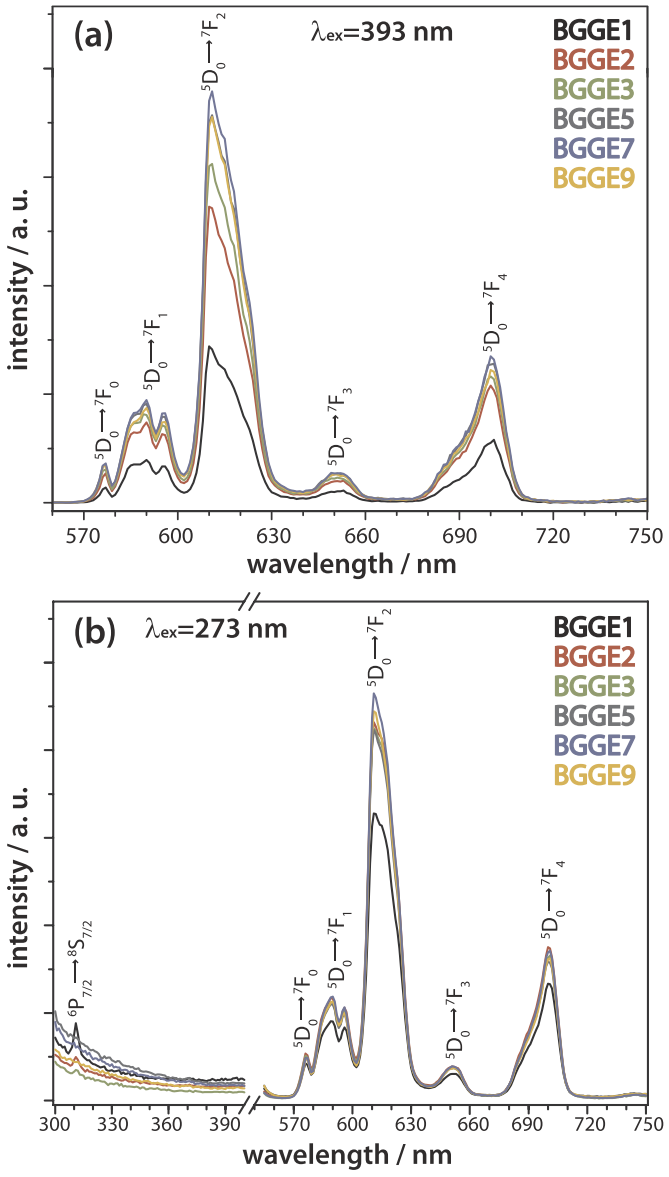

Fig. 5. Emission spectra of BGGEx glasses excited under 393 nm (a) and 273 nm (b).

excitation spectra of BGGEx glasses belongs to the transition at 393 nm. Fig. 4 also illustrates that all excitation peaks become more intense up to x = 7 mol% and then weaken due to concentration quenching at x = 9 mol%.

The emission spectra of BGGEx glasses have been measured by exciting at 393 nm in the wavelength range from 560 to 750 nm as shown in Fig. 5(a). The emission of Eu^{3+} arises from transitions between 4f–4f levels and is principally due to electric dipole or magnetic dipole interactions. The emission bands of Eu^{3+} ions can be assigned to $^5D_0 \rightarrow {}^7F_0$ (575 nm), $^5D_0 \rightarrow {}^7F_1$ (593 nm), $^5D_0 \rightarrow {}^7F_2$ (610 nm), $^5D_0 \rightarrow {}^7F_3$ (650 nm), and $^5D_0 \rightarrow {}^7F_4$ (700 nm) transitions [38]. It can be seen that the characteristic emission intensities of Eu^{3+} ions go up rapidly, reach the highest value for x = 7 mol% and then decrease due to concentration quenching. The strongest red emission, hypersensitive to the environment, is the electric dipole transition $^5D_0 \rightarrow {}^7F_2$ at 610 nm and follows the selection rule of ΔJ = 2. Besides this, the $^5D_0 \rightarrow {}^7F_1$ (593 nm) transition which is independent of local symmetry have magnetic dipole character and follows the selection rule of ΔJ = 1 [39]. The ratio of integrated emission intensity of the $^5D_0 \rightarrow {}^7F_2$ transition to the $^5D_0 \rightarrow {}^7F_1$ transition is defined as red to orange ratio (R/O, also called as asymmetric ratio) obtained to estimate the local symmetry around the Eu^{3+} ions [40,41]. As can be seen from Table 3, R/O values increase linearly with the Eu^{3+} doping level indicating that the environment of Eu^{3+} ions are becoming more asymmetric.

Table 3
Asymmetric ratio (R/O), J-O parameters (Ω_2 and Ω_4), total radiative decay rate (A_{rad}), radiative decay time (τ_{rad}), and emission efficiency (η) of BGGEx glasses.

	BGGE1	BGGE2	BGGE3	BGGE5	BGGE7	BGGE9
R/O	3.54	3.64	3.71	3.82	3.91	3.99
Ω_2 (x10^{-20} cm^2)	5.54	5.69	5.84	6.04	6.18	6.30
Ω_4 (x10^{-20} cm^2)	4.45	4.50	4.40	4.47	4.42	4.42
A_{rad} (s^{-1})	4.63	4.81	4.73	4.75	4.89	4.85
τ_{rad} (s)	2.16	2.08	2.11	2.10	2.04	2.06
η (%)	71.6	75.3	72.2	70.6	71.1	66.7

Energy transfer from Gd^{3+} to Eu^{3+} ions were studied by obtaining the emission spectra of BGGEx glasses under 273 nm ($^8S_{7/2}$-$^6I_{11/2}$ for Gd^{3+} ion) excitation as illustrated in Fig. 5(b). The radiative transition of Gd^{3+} ion at 311 nm has maximum intensity and sharpness for x = 1 mol% [20]. In general, doping level has an effect on luminescent properties and energy transfer mechanism [42]. So it can be concluded that with the elevated concentration of Eu^{3+} ions the decrease in the emission intensity of Gd^{3+} at 311 nm and the increase in the characteristic emission intensities of Eu^{3+} ion may demonstrate energy transfer from Gd^{3+} to Eu^{3+}. When the Gd^{3+} ions spend all of their energy by transferring it to the neighboring Eu^{3+} activators, concentration quenching of luminescence occurs [43].

The critical distances (R_c) for Gd^{3+}–Eu^{3+} and Eu^{3+}–Eu^{3+} ion pairs for the optimum concentration were calculated to be 4.622 and 7.512 Å, respectively as given in Table 1. The obtained distances are greater than 4 Å indicating that the dominant mechanism of concentration quenching for BGGEx glasses is multipolar interaction [44]. Furthermore, it is found that the shorter related ion separations will quench Gd^{3+} (Eu^{3+}) emission, as shown in Fig.5(b).

3.4. Judd-Ofelt analysis

The Judd-Ofelt analysis on the PL emission spectrum is used to gain knowledge about local structure and chemical bonding of rare-earth ions in host material [45,46]. The Ω_J (J = 2, 4 and 6) J-O parameters can be obtained from the ratio of the integrated emission intensities of corresponding transitions as follows:

$$\Omega_J = \frac{S[^5D_0 \rightarrow {}^7F_J]}{S[^5D_0 \rightarrow {}^7F_1]}\left(\frac{\nu[^5D_0 \rightarrow {}^7F_1]}{\nu[^5D_0 \rightarrow {}^7F_J]}\right)^3 \frac{S_{md}}{e^2}\frac{9n^2}{(n^2+2)^2}[\langle {}^5D_0 \mid U^{(\lambda)} \mid {}^7F_J\rangle^2]^{-1}$$

$S[^5D_0 \rightarrow {}^7F_J]$ and $\nu[^5D_0 \rightarrow {}^7F_J]$ are the integrated emission intensities and wavenumbers of the transitions from $^5D_0$ excited state to the low-lying ^7F_J states (J = 0,1,...,6), respectively. e is the electric charge and $[9n^2/(n^2+2)^2]$ is the Lorentz local field correction factor in terms of refraction index (n). The values of square reduced matrix elements, $\langle {}^5D_0 \mid U^{(\lambda)} \mid {}^7F_J\rangle^2$, are not affected from the chemical environment of Eu^{3+} ion and are taken from Carnall et al. [33] (0.0032, 0.0023 and 0.0002 for λ = 2,4 and 6, respectively). S_{md}, the magnetic dipole line strength value of $^5D_0 \rightarrow {}^7F_1$ transition, is also obtained from the literature [47]. The $^5D_0 \rightarrow {}^7F_6$ transition which lies in the near infrared region could not be observed in BGGEx glass due to the experimental limitations.

The total radiative decay rate, A_{rad}, can be expressed in terms of the radiative decay rates of each $^5D_0$ to ^7F_J (J = 0,1,...,6) transition

$$A_{rad} = \sum_{J=0}^{6} A_{rad}[^5D_0 \rightarrow {}^7F_J]$$

As mentioned before, J = 1 and J = 2, 4 transitions are conducted only by magnetic and electric dipole mechanisms, respectively, while the remaining ones (J = 0, 3, 5) have both electric and magnetic

contributions. Due to very low intensities, J = 0, 3, 5 transitions can be neglected [48]. The radiative decay rate can be written as electric and magnetic dipole parts:

$$A_{rad}[^5D_0 \rightarrow {}^7F_J] = \frac{64\pi^4}{3h(2J+1)}(\nu[^5D_0 \rightarrow {}^7F_J])^3\left[\frac{n(n^2+2)^2}{9}S_{ed} + n^3 S_{md}\right]$$

where h is Planck constant and (2J + 1) is the degeneracy of the initial state. The electric dipole line strength (S_{ed}) is given by

$$S_{ed} = e^2 \sum_{\lambda=2,4,6} \Omega_\lambda \langle {}^5D_0 \mid U^{(\lambda)} \mid {}^7F_J \rangle^2$$

The radiative decay time, $\tau_{rad} = 1/A_{rad}$, is the inverse of the total radiative decay rate. Using experimental decay time values (τ_{exp}), the non-radiative decay time (τ_{nrad}) can be calculated from

$$\frac{1}{\tau_{nrad}} = \frac{1}{\tau_{exp}} - \frac{1}{\tau_{rad}}$$

Finally, the emission efficiency (η) is given by

$$\eta = \frac{\tau_{exp}}{\tau_{rad}}$$

The J-O parameters (Ω_2, Ω_4), total radiative decay rates (A_{rad}), radiative (τ_{rad}) and non- radiative (τ_{nrad}) decay times and the emission efficiencies (η) for Eu^{3+} doped borogermanate glasses have been calculated and tabulated in Table 3. In BGGEx glasses the Ω_2 values increase with increasing Eu^{3+} content which indicates the Eu-O bond having more covalent character. Beside this Ω_4 value does not affected by the change in Eu^{3+} concentration.

The same behaviors in J-O parameters such as linear relation between Ω_2 and doping level and secondly $\Omega_2 > \Omega_4$ have also been observed for various other europium doped glasses such as borogermanate [11,49], telluroborate [50] and tellurite [51]. This is the evidence of the covalent character of interaction between the Eu^{3+} ions and surrounding ligands.

3.5. Luminescence decay curve

Luminescence decay time measurements are very convenient for determining the energy transfer mechanism and luminescence quenching behavior. Fig. 6(a) presents the decay time measurements of Gd^{3+} $^6P_{7/2} \rightarrow {}^8S_{7/2}$ transition (311 nm) excited at 273 nm in BGGEx glasses. As can be seen from the figure that the curve does not show exponential behavior therefore decay time was taken as corresponding time at where luminescence intensity has e^{-1} of its initial value. The decreasing decay time of Gd^{3+} $^6P_{7/2} \rightarrow {}^8S_{7/2}$ transition with increasing Eu^{3+} ion concentration is proof of higher energy transfer from Gd^{3+} to Eu^{3+} ions.

The effect of Eu^{3+} concentration on decay times of $^5D_0$–$^7F_2$ (610 nm) transition under 273 nm excitation is shown in Fig. 6(b). The luminescence decay time curves of BGGEx glasses well fitted with two-exponential components.

Upon the increase in x values, the decay times reduce and after concentration quenching at x = 7 mol% its decrease becomes more rapid. Variations in luminescence decay time occur due to self-generated quenching that happen between Eu^{3+} ions in the host [52].

4. Conclusion

Borogermanate glasses in the B_2O_3-GeO_2-Gd_2O_3 ternary system have been prepared by melt quenching method and their physical, optical and luminescent properties were investigated as a function of Eu^{3+} ion concentration. These glasses measured densities up to 4.824 g/cm^3 are due to the presence of heavy Gd^{3+} element in the glass network. The glasses exhibited a high transparency of about 80% in the 440 to 900 nm region. It was also found that the optical band gaps evaluated from the absorption spectra can be narrowed by increasing

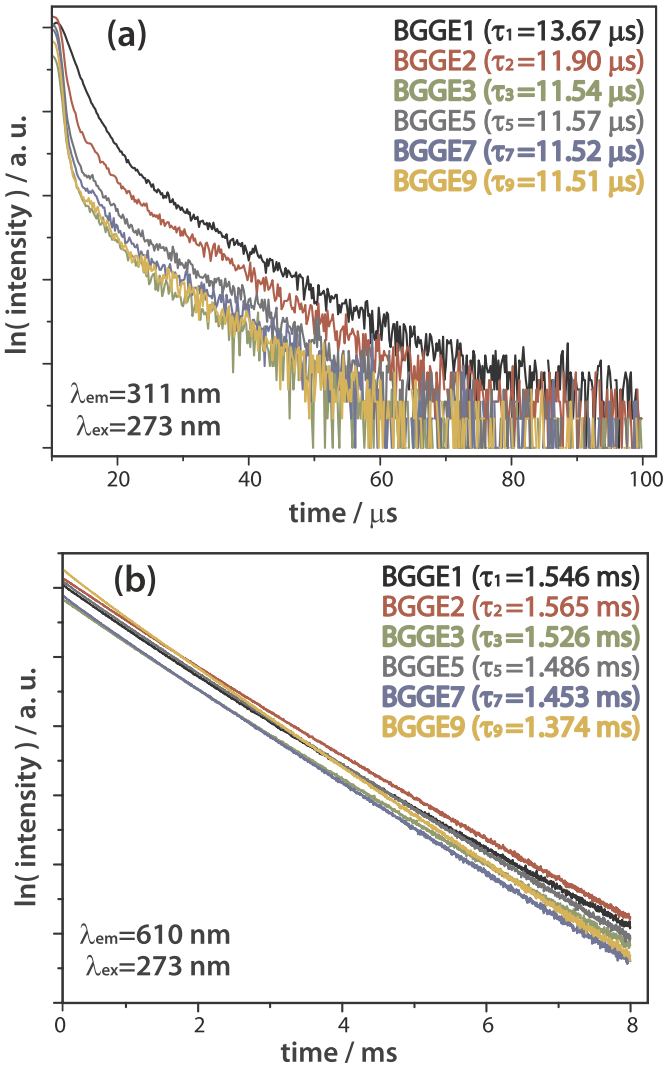

Fig. 6. Luminescence decay time curves of (a) Gd^{3+} (monitoring the PL peak of Gd^{3+} at 311 nm) and (b) Eu^{3+} (monitoring the PL peak of Eu^{3+} at 610 nm) in BGGEx glasses under 273 nm excitation, respectively.

content of Eu^{3+}. This effect was found to have a correlation with the changes in the glass structure where the addition of Eu^{3+} to the glass network is known to create non-bridging oxygen. The energy transfer process from Gd^{3+} to Eu^{3+} ions in Eu^{3+} doped borogermanate glasses has been identified based on emission and excitation spectra and luminescence decay curves. The energy transfer efficiency from Gd^{3+} to Eu^{3+} reached 75% when the content of Eu^{3+} was greater than 1 mol%. Judd-Ofelt parameters were evaluated from the emission spectrum. For all BGGEx glasses, J-O parameter Ω_2 have been found to be greater than Ω_4, which provides evidence of the covalent character of interaction between the Eu^{3+} ions and surrounding ligands. Moreover, this correlation between the increment of Ω_2 and concentration of Eu^{3+} ions suggests increased Eu–O covalency and more distortion of the local symmetry. The results obtained from this study are thought to be of value in furthering studies on Eu^{3+} doped borogermanate glasses and imply that the these glasses are of significance for scintillating applications.

Acknowledgments

We wish to express our gratitude to the financial support provided by The Scientific and Technological Research Council of Turkey (TÜBİTAK, Project number: 114M477).

References

[1] E. Álvarez, M.E. Zayas, J.A. Rivera, F.F. Domínguez, R.P.D. Zamorano, U. Caldiño, New reddish-orange and greenish-yellow light emitting phosphors: Eu^{3+} and Tb^{3+}/Eu^{3+} in sodium germanate glass, J. Lumin. 153 (2014) 198–202.

[2] I. Iparraguirre, J. Azkargorta, J.M. Fernandez-Navarro, M. Al-Saleh, J. Fernandez, R. Balda, Laser action and upconversion of Nd^{3+} in tellurite bulk glass, J. Non-Cryst. Solids 353 (2007) 990.

[3] S. Tanabe, Rare-earth-doped glasses for fiber amplifiers in broadband telecommunication, C. R. Chimie 5 (2002) 815–824.

[4] G.S. Maciel, C.B.D. Arau, Y. Messaddeq, M.A. Aegerter, Frequency upconversion in Er^{3+} doped fluoroindate glasses pumped at 1.48 mm, Phys Rev B 55 (10) (1997) 6335–6342.

[5] K. Marimuthu, R.T. Karunakaran, S.S. Babu, G. Muralidharan, S. Arumugam, C.K. Jayasankar, Structural and spectroscopic investigations on Eu^{3+} doped alkali fluoroborate glasses, Solid State Sci 11 (2009) 1297–1302.

[6] S.A. Dalhatu, R. Hussin, K. Deraman, Structural and luminescence properties of Eu^{3+} doped magnesium sulfide borate glass and crystal, Chin. J. Phys. 54 (2016) 877–882.

[7] U. Caldiño, G. Muñoz, H.I. Camarillo, A. Speghini, M. Bettinelli, Down-shifting by energy transfer in Tb^{3+}/Dy^{3+} codoped zinc phosphate glasses, J. Lumin. 161 (2015) 142–146.

[8] Z. Wu, B. Chen, X. Li, J. Zhang, J. Sun, H. Zhong, H. Zheng, L. Tong, H. Xia, Optical transition properties, energy transfer mechanism and luminescent thermal stability of Sm^{3+} doped silicate glasses, J. Alloy Compd. 663 (2016) 545–551.

[9] C. Zuo, A. Xiao, Z. Zhou, Y. Chen, X. Zhang, X. Ding, X. Wang, Q. Ge, Spectroscopic properties of Ce^{3+} doped BaO-Gd_2O_3-Al_2O_3-B_2O_3-SiO_2 glasses, J. Non-Cryst. Solids 452 (2016) 35–39.

[10] X.Y. Sun, D.G. Jiang, S.W. Chen, G.T. Zheng, S.M. Huang, M. Gu, Z.J. Zhang, J.T. Zhao, Eu^{3+} activated borogermanate scintillating glass with a high Gd_2O_3 content, J. Am. Ceram. Soc. 96 (5) (2013) 1483–1489.

[11] X. Liu, Y. Qiao, G. Dong, S. Ye, B. Zhu, G. Lakshminarayana, D. Chen, J. Qiu, Cooperative downconversion in Yb^{3+}–RE^{3+} (RE = Tm or Pr) codoped lanthanum borogermanate glasses, Opt. Lett. 33 (23) (2008) 2858–2860.

[12] G.E. Malashkevich, V.N. Sigaev, N.V. Golubev, V.I. Savinkov, P.D. Sarkisov, I.A. Khodasevich, V.I. Dashkevich, A.V. Mudryi, Luminescence of borogermanate glasses activated by Er^{3+} and Yb^{3+} ions, J. Non-Cryst. Solids 357 (2011) 67–72.

[13] Z. Na, K.N. Sharafudeen, D. Guoping, P. Mingying, Q. Jianrong, Mixed network effect of broadband near-infrared emission in bi-doped B_2O_3-GeO_2 glasses, J. Am. Ceram. Soc. 95 (12) (2012) 3842–3846.

[14] J. Rajagukguk, J. Kaewkhao, M. Djamal, R. Hidayat, Suprijadi, Y. Ruangtaweep, Structural and optical characteristics of Eu^{3+} ions in sodium-leadzinc-lithium-borate glass system, J. Mol. Struct. 1121 (2016) 180–187.

[15] X.Y. Sun, D.G. Jiang, W.F. Wang, C.Y. Cao, Y.N. Li, G.T. Zhen, H. Wang, X.X. Yang, H.H. Chen, Z.J. Zhang, J.T. Zhao, Luminescence properties of B_2O_3–GeO_2–Gd_2O_3 scintillating glass doped with rare-earth and transition-metal ions, Nucl. Instrum. Meth. A 716 (2013) 90–95.

[16] X.Y. Sun, W.F. Wang, X.G. Yu, Y.N. Li, X.X. Yang, H.H. Chen, Z.J. Zhang, J.T. Zhao, Luminescent properties of Eu^{3+} activated (70-x)B_2O_3-xGeO_2-Gd_2O_3 scintillating glasses, IEEE Trans. Nucl. Sci. 61 (1) (2014) 380–384.

[17] X.Y. Sun, D.G. Jiang, Y.Z. Suna, X. Zhang, Q.L. Hu, Y. Huang, Y. Tao, Eu^{3+} activated B_2O_3–GeO_2–RE_2O_3 (RE = Y^{3+}, La^{3+} and Gd^{3+}) borogermanate scintillating glasses, J. Non-Cryst. Solids 389 (2014) 72–77.

[18] Y. Gandhi, P. Rajanikanth, M.S. Rao, V.R. Kumar, N. Veeraiah, M. Piasecki, Effect of tin ions on enhancing the intensity of narrow luminescence line at 311 nm of Gd^{3+} ions in Li_2O-PbO-P_2O_5 glass system, Opt. Mater. 57 (2016) 39–44.

[19] W. Chewpraditkul, X. He, D. Chen, Y. Shen, Q. Sheng, B. Yu, M. Nikl, R. Kucerkova, A. Beitlerova, C. Wanarak, A. Phunpueok, Luminescence and scintillation of Ce^{3+}-doped oxide glass with high Gd_2O_3 concentration, Phys. Status Solidi 208 (12) (2011) 2830–2832.

[20] D. He, C. Yu, J. Cheng, S. LI, L. Hu, Energy transfer between Gd^{3+} and Tb^{3+} in phosphate glass, J. Rare Earth. 29 (1) (2011) 48–51.

[21] Y. Zhang, J. Lv, N. Ding, S. Jiang, T. Zheng, J. Li, Tunable luminescence and energy transfer from Gd^{3+} to Tb^{3+} ions in silicate oxyfluoride scintillating glasses via varying Tb^{3+} concentration, J. Non-Cryst. Solids 423–424 (2015) 30–34.

[22] C.R. Kesavulu, H.J. Kim, S.W. Lee, J. Kaewkhao, E. Kaewnuam, N. Wantana, Luminescence properties and energy transfer from Gd^{3+} to Tb^{3+} ions in gadolinium calcium silicoborate glasses for green laser application, J. Alloy Compd. 704 (2017) 557–564.

[23] N. Wantana, S. Kaewjaeng, S. Kothan, H.J. Kim, J. Kaewkhao, Energy transfer from Gd^{3+} to Sm^{3+} and luminescence characteristics of CaO–Gd_2O_3–SiO_2–B_2O_3 scintillating glasses, J. Lumin. 181 (2017) 382–386.

[24] J. Kaewkhao, N. Wantana, S. Kaewjaeng, S. Kothan, H.J. Kim, Luminescence characteristics of Dy^{3+} doped Gd_2O_3-CaO-SiO_2-B_2O_3 scintillating glasses, J. Rare Earth 34 (6) (2016) 583–589.

[25] F. Zaman, G. Rooh, N. Srisittipokakun, H.J. Kim, E. Kaewnuam, P. Meejitpaisan, J. Kaewkhao, Scintillation and luminescence characteristics of Ce^{3+} doped in Li_2O–Gd_2O_3–BaO–B_2O_3 scintillating glasses, Radiat. Phys. Chem. 130 (2017) 158–163.

[26] J. Fu, M. Kobayashi, S. Sugimoto, J.M. Parker, Eu^{3+} activated heavy scintillating glasses, Mater. Res. Bull. 43 (2008) 1502–1508.

[27] X.Y. Liu, H. Guo, S.X. Dai, M.Y. Peng, Q.Y. Zhang, Energy transfer and thermal stability in Bi^{3+}/Eu^{3+} co-doped germanium-borate glasses for organic-resin-free UV LEDs, Opt. Mater. Express 6 (11) (2016) 3574–3585.

[28] J.S. McCloy, Methods for prediction of refractive index in glasses for the infrared, SPIE Proc. 8016 (2011) 1–16.

[29] A. Hoaksey, J. Woods, K.N.R. Taylor, Luminescence of Tb^{3+} ions in silicate glasses, J. Lumin. 17 (1978) 385–400.

[30] B. Bhatia, S.L. Meena, V. Parihar, M. Poonia, Optical basicity and polarizability of Nd^{3+}-doped bismuth borate glasses, N. J. Glass Ceram. 5 (2015) 44–52.

[31] N. Zhang, K.N. Sharafudeen, G. Dong, M. Peng, J. Qiu, Mixed network effect of broadband near-infrared emission in Bi-Doped glasses, J. Am. Ceram. Soc. 95 (12) (2012) 3842–3846.

[32] N. Zhang, J. Qiu, G. Dong, Z. Yang, Q. Zhang, M. Peng, Broadband tunable near-infrared emission of Bi-doped composite germanosilicate glasses, J. Mater. Chem. 22 (7) (2012) 3154–3159.

[33] W.T. Carnall, P.R. Fields, K. Rajnak, Electronic energy levels of the trivalent lanthanide aquo ions. IV. Eu^{3+}, J. Chem. Phys. 49 (1968) 4450–4455.

[34] X.Y. Sun, Z.P. Ye, Z.J. Zhang, L.W. Liu, D.P. Chen, J.T. Zhao, Energy transfer study on dense Eu^{3+}/Tb^{3+} coactivated oxyfluoride borogermanate scintillating glasses, J. Am. Ceram. Soc. 98 (3) (2015) 781–787.

[35] J. Tauc, A. Menth, States in the gap, J. Non-Cryst. Solids 8–10 (1972) 569–584.

[36] J.C. Krupa, I. Gerard, A. Mavolet, Electronic structure of f–element systems in the Uv and Vuv energy range, Acta Phys. Pol. A 84 (1993) 843–848.

[37] K.W. Meert, V.A. Morozov, A.M. Abakumov, J. Hadermann, D. Poelman, P.F. Smet, Energy transfer in Eu^{3+} doped scheelites: use as thermographic phosphor, Opt. Express 22 (2014) A961–A972.

[38] W.T. Carnall, P.R. Fields, K. Rajnak, Spectral intensities of the trivalent lanthanides and actinides in solution. II. Pm^{3+}, Sm^{3+}, Eu^{3+}, Gd^{3+}, Tb^{3+}, Dy^{3+}, and Ho^{3+}, J. Chem. Phys. 49 (1968) 4412–4423.

[39] H. Yang, J. Shi, M. Gong, H. Liang, A novel red phosphor: Ca_2GeO_4:Eu^{3+}, J. Rare Earth 28 (4) (2010) 519–522.

[40] L. Zur, Structural and luminescence properties of Eu^{3+}, Dy^{3+} and Tb^{3+} ions in lead germanate glasses obtained by conventional high-temperature melt-quenching technique, J. Mol. Struct. 1041 (2013) 50–54.

[41] J. Kaewkhaoa, K. Boonin, P. Yasaka, H.J. Kim, Optical and luminescence characteristics of Eu^{3+} doped zinc bismuth borate (ZBB) glasses for red emitting device, Mater. Res. Bull. 71 (2015) 37–41.

[42] N. Liu, J.Y. Si, G.M. Cai, Y. Tao, Crystal structure, luminescent properties and energy transfer of Eu^{3+}/Dy^{3+} doped $GdNbTiO_6$ broad band excited phosphors, RSC Adv. 6 (2016) 50797–50807.

[43] G. Blasse, Energy transfer in oxidic phosphors, Philips Res. Rep. 28 (6) (1968) 444–445.

[44] F. Yang, Y. Liang, M. Liu, X. Li, M. Zhang, N. Wang, Photoluminescence properties of novel red-emitting NaSrBO3:Eu^{3+} phosphor for near-UV light-emitting diodes, Opti. Laser Technol 46 (2013), pp. 14–19.

[45] B.R. Judd, Optical absorption intensities of rare-earth ions, Phys. Rev. 127 (1962) 750–761.

[46] G.S. Ofelt, Intensities of crystal spectra of rare earth ions, J. Chem. Phys. 37 (1962) 511–520.

[47] M.J. Weber, T.E. Varitimo, B.H. Matsinge, Optical intensities of rare-earth ions in yttrium orthoaluminate, Phys. Rev. B 8 (1973) 47.

[48] N.B.D. Lima, J.D.L. Dutra, S.M.C. Gonçalves, R.O. Freire, A.M. Simas, Chemical partition of the radiative decay rate of luminescence of Europium complexes, Sci. Rep. 6 (2016) 21204–21216.

[49] X.Y. Sun, X. Zhang, H.H. Chen, Q.L. Hu, W.F. Wang, Z.J. Zhang, J.T. Zhao, Investigation on the luminescent properties of Eu^{3+} activated dense oxyfluoride borogermanate scintillating glasses, J. Non-Cryst. Solids 404 (2014) 162–166.

[50] K. Annapoorani, K. Marimuthu, Spectroscopic properties of Eu^{3+} ions doped Barium telluroborate glasses for red laser applications, J. Non-Cryst. Solids 463 (2017) 148–157.

[51] W. Stambouli, H. Elhouichet, B. Gelloz, M. Ferid, Optical and spectroscopic properties of Eu-doped tellurite glasses and glass ceramics, J. Lumin. 138 (2013) 201–208.

[52] K.K. Rasu, D. Balaji, S.M. Babu, Spectroscopic properties of Eu^{3+}:$KLa(WO_4)_2$ novel red phosphors, J. Lumin. 170 (2016) 547–555.